

Photoexcitation of Na Bose-Einstein condensates

M. S. Pindzola, Sh. A. Abdel-Naby, and F. Robicheaux

Department of Physics, Auburn University, Auburn, Alabama 36849, USA

(Received 24 August 2012; published 5 November 2012)

The photoexcitation of Na Bose-Einstein condensates is studied by direct solution of the Gross-Pitaevskii equation in both cylindrical and Cartesian coordinates. As the frequency of a Bragg scattering potential is varied the first dipole mode of the ground state is brought into resonance. The dipole mode frequency is verified by diagonalization of the Bogoliubov–de Gennes matrix in cylindrical coordinates. Dipole mode frequencies are found for Na condensates bound in both isotropic and nonisotropic magnetic traps.

DOI: [10.1103/PhysRevA.86.055601](https://doi.org/10.1103/PhysRevA.86.055601)

PACS number(s): 03.75.Hh, 32.80.Fb

I. Introduction. Photoexcitation has played a vital role in the understanding of atomic and molecular structure. Over the years, the photoexcitation of excited states has progressed from an understanding of low-lying bound states to resonance bound states embedded in the continuum. For example, the R -matrix method [1] has been used quite successfully to map out complicated resonance structures in the photoionization of many atoms and small molecules. Recently, R -matrix calculations have been performed for the photoionization of N [2] and of both N_2 and NO [3].

Photoexcitation is beginning to play a role in the understanding of the complex excited state structure of Bose-Einstein condensates. Solution of the Gross-Pitaevskii [4,5] equation with the inclusion of a Bragg scattering potential [6,7] has provided a means to search for vortices and to better understand the rich excited mode spectrum. Recent experiments [8–10] have begun to map out photoexcitation resonances of condensates using Bragg spectroscopy. Bragg spectroscopy has also been used to photoionize condensates to study scattering by distinct colliding condensate wave packets [11,12].

Recently [13], we calculated the collective modes of Bose-Einstein condensates by diagonalization of the Bogoliubov–de Gennes matrix [14–16] in cylindrical coordinates. We also checked our matrix solution by solving the Gross-Pitaevskii equation with the inclusion of a radial time-dependent potential in both cylindrical and Cartesian coordinates to obtain the lowest breathing modes. In this article, we solve the Gross-Pitaevskii equation with the inclusion of a Bragg scattering potential to search for dipole modes of Na Bose-Einstein condensates found in isotropic and nonisotropic magnetic traps. The dipole mode frequencies are verified by diagonalization of the Bogoliubov–de Gennes matrix.

This article is organized as follows. We present the time-dependent Gross-Pitaevskii equation and the Bogoliubov–de Gennes matrix in Sec. II. We present results for the photoexcitation of Na condensates in both isotropic and nonisotropic magnetic traps in Sec. III. A brief summary is found in Sec. IV.

II. Theory. The ground and excited states of a Bose-Einstein condensate may be found by relaxation of the Gross-Pitaevskii (GP) equation in imaginary time ($\tau = it$):

$$-\hbar \frac{\partial \Psi(\vec{r}, \tau)}{\partial \tau} = [H(\vec{r}) + V(\vec{r}, \tau)]\Psi(\vec{r}, \tau), \quad (1)$$

where

$$H(\vec{r}) = -\frac{\hbar^2}{2m} \nabla^2 + V_{\text{trap}}(\vec{r}), \quad (2)$$

m is the mass of the atom, and $\Psi(\vec{r}, \tau)$ is normalized to 1. A general harmonic trap potential is given by

$$V_{\text{trap}}(\vec{r}) = \frac{1}{2}m(\vec{\omega} \cdot \vec{r})^2, \quad (3)$$

where $\vec{\omega}$ is the trap frequency ($f = \omega/2\pi$ in Hz). The nonlinear potential is given by

$$V(\vec{r}, \tau) = \frac{4\pi\hbar^2 a N}{m} |\Psi(\vec{r}, \tau)|^2, \quad (4)$$

where a is the scattering length and N is the number of atoms.

The photoexcitation of Bose-Einstein condensates may be studied by propagation of the GP equation in real time:

$$i\hbar \frac{\partial \Psi(\vec{r}, t)}{\partial t} = [H(\vec{r}) + V(\vec{r}, t) + V_B(\vec{r}, t)]\Psi(\vec{r}, t). \quad (5)$$

The Bragg scattering potential is given by

$$V_B(\vec{r}, t) = A_B(t) \cos(\vec{q}_L \cdot \vec{r} - \omega_L t), \quad (6)$$

where $A_B(t)$ is a time-varying amplitude, \vec{q}_L is a two-laser wave vector difference, and ω_L is a two-laser frequency difference.

The set of collective modes for a ground-state solution, $\Psi_0(\vec{r})$, with an energy E_0 , as determined by relaxation of Eq. (1), may be found by diagonalization of the Bogoliubov–de Gennes (BdG) matrix given by

$$M_{\text{BdG}} = \begin{pmatrix} H(\vec{r}) + 2V_0(\vec{r}) - E_0 & V_0(\vec{r}) \\ -V_0(\vec{r}) & -H(\vec{r}) - 2V_0(\vec{r}) + E_0 \end{pmatrix}, \quad (7)$$

where

$$V_0(\vec{r}) = \frac{4\pi\hbar^2 a N}{m} |\Psi_0(\vec{r})|^2. \quad (8)$$

The wave function for a Bose-Einstein condensate may be expressed in scaled cylindrical coordinates:

$$\Psi(\vec{r}, t) = \frac{P(\rho, z, t)}{\sqrt{\rho}} \frac{e^{im_l \phi}}{\sqrt{2\pi}}, \quad (9)$$

where the spatial scaling factor is $l = \sqrt{\hbar/m\omega_\rho}$ and the energy scaling factor is $\hbar\omega_\rho$. For the ground state of the condensate we choose $m_l = 0$. Using lattice techniques [13] to obtain a discrete representation of the wave function and associated operators on a two-dimensional uniform grid, the GP equation

in real time becomes

$$i \frac{\partial P(\rho_i, z_j, t)}{\partial t} = -\frac{1}{2} \left(\frac{c_i^+ P(\rho_{i+1}, z_j, t) + c_i^- P(\rho_{i-1}, z_j, t) - 2P(\rho_i, z_j, t)}{\Delta \rho^2} \right) - \frac{1}{2} \left(\frac{P(\rho_i, z_{j+1}, t) + P(\rho_i, z_{j-1}, t) - 2P(\rho_i, z_j, t)}{\Delta z^2} \right) + \frac{1}{2} (\rho_i^2 + \lambda^2 z_j^2) P(\rho_i, z_j, t) + 4\pi Q \frac{|P(\rho_i, z_j, t)|^2}{2\pi \rho_i} P(\rho_i, z_j, t) + \bar{A}_B(t) \cos(\bar{q}_L z_j - \bar{\omega}_L t) P(\rho_i, z_j, t), \quad (10)$$

where $c_i^+ = \frac{\rho_{i+\frac{1}{2}}}{\rho_i \rho_{i+1}}$, $c_i^- = \frac{\rho_{i-\frac{1}{2}}}{\rho_i \rho_{i-1}}$, $\lambda = \frac{\omega_z}{\omega_\rho}$, $Q = \frac{aN}{l}$, $\bar{A}_B = \frac{A_B}{\hbar \omega_\rho}$, $\bar{q}_L = \frac{q_L}{l}$, and $\bar{\omega}_L = \frac{\omega_L}{\omega_\rho}$. Similar lattice expressions may also be obtained for the GP equation in imaginary time and the BdG matrix.

The wave function for a Bose-Einstein condensate may also be expressed in scaled Cartesian coordinates:

$$\Psi(\vec{r}, t) = P(x, y, z, t), \quad (11)$$

where the spatial scaling factor is $l = \sqrt{\hbar/m\omega_x}$ and the energy scaling factor is $\hbar\omega_x$. Using lattice techniques, the GP equation in real time becomes

$$i \frac{\partial P(x_i, y_j, z_k, t)}{\partial t} = -\frac{1}{2} \left(\frac{P(x_{i+1}, y_j, z_k, t) + P(x_{i-1}, y_j, z_k, t) - 2P(x_i, y_j, z_k, t)}{\Delta x^2} \right) - \frac{1}{2} \left(\frac{P(x_i, y_{j+1}, z_k, t) + P(x_i, y_{j-1}, z_k, t) - 2P(x_i, y_j, z_k, t)}{\Delta y^2} \right) - \frac{1}{2} \left(\frac{P(x_i, y_j, z_{k+1}, t) + P(x_i, y_j, z_{k-1}, t) - 2P(x_i, y_j, z_k, t)}{\Delta z^2} \right) + \frac{1}{2} (x_i^2 + \lambda_1^2 y_j^2 + \lambda_2^2 z_k^2) P(x_i, y_j, z_k, t) + 4\pi Q |P(x_i, y_j, z_k, t)|^2 P(x_i, y_j, z_k, t) + \bar{A}_B(t) \cos(\bar{q}_L z_k - \bar{\omega}_L t) P(x_i, y_j, z_k, t), \quad (12)$$

where $\lambda_1 = \frac{\omega_y}{\omega_x}$ and $\lambda_2 = \frac{\omega_z}{\omega_x}$. A similar lattice expression may also be obtained for the GP equation in imaginary time.

III. Results. We searched for the lowest energy dipole mode of a Na condensate with an atomic scattering length of $a = 2.9$ nm and the number of atoms $N = 4400$. We chose a fairly small number of atoms to keep the kinetic energy term of Eq. (2) and the nonlinear potential of Eq. (4) to be of roughly equal importance. In cylindrical coordinates we chose $f_\rho = 25$ Hz for the magnetic trap, resulting in a length scaling factor of $l = 4.19 \times 10^{-4}$ cm and an energy scaling factor of $\hbar\omega_\rho = 1.03 \times 10^{-13}$ eV (1.20 nK). We employed a 50×100 point numerical lattice with $\rho = 0.0 \rightarrow +10.0$ with $\Delta\rho = 0.20$ and $z = -10.0 \rightarrow +10.0$ with $\Delta z = 0.20$.

Upon relaxation of the GP equation in imaginary time for an isotropic magnetic trap with $f_\rho = 25$ Hz and $f_z = 25$ Hz, we obtained a ground state with energy $E_0 = 2.74$. We then propagated the GP equation in real time, as given by Eq. (10). The time-dependent amplitude for the Bragg scattering potential is given by

$$\bar{A}_B(t) = \bar{A} \sin^2(\pi t/2T) \quad \text{for } 0 < t < T, \quad (13)$$

$$\bar{A}_B(t) = \bar{A} \quad \text{for } T < t < 9T, \quad (14)$$

$$\bar{A}_B(t) = \bar{A} \sin^2[\pi(10T - t)/2T] \quad \text{for } 9T < t < 10T, \quad (15)$$

where $\bar{A} = 0.3$ and $T = 2\pi/\bar{\omega}_L$. For $\bar{q}_L = 1.0$, we varied the Bragg scattering frequency $\bar{\omega}_L$ from 0.9 to 1.1 while keeping track of the energy given by

$$E(t) = \langle \Psi(\vec{r}, t) | H(\vec{r}) + V(\vec{r}, t) + V_B(\vec{r}, t) | \Psi(\vec{r}, t) \rangle. \quad (16)$$

We present the results for $E(5T)$ and $E(10T)$ as a function of $\bar{\omega}_L$ in Fig. 1. Clearly, there is a resonance around $\bar{\omega}_L = 1.0$, and the energy becomes more sharply peaked for longer pulse durations.

In Cartesian coordinates, we chose an isotropic magnetic trap with $f_x = f_y = f_z = 25$ Hz. We employed a $100 \times 100 \times 100$ point numerical lattice with $x = -10.0 \rightarrow +10.0$ with $\Delta x = 0.20$, $y = -10.0 \rightarrow +10.0$ with $\Delta y = 0.20$, and $z = -10.0 \rightarrow +10.0$ with $\Delta z = 0.20$. Upon relaxation of the GP equation in imaginary time, we again obtained a ground state

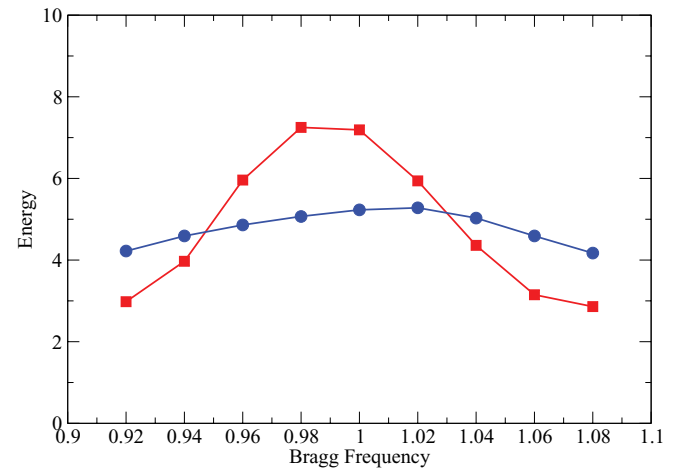


FIG. 1. (Color online) Photoexcitation of a Na condensate in an isotropic magnetic trap with $f_\rho = 25$ Hz and $f_z = 25$ Hz. Circles: Energy at $t = 5T$. Squares: Energy at $t = 10T$ (energies and frequencies are in scaled units of $\hbar\omega_\rho = 1.03 \times 10^{-13}$ eV).

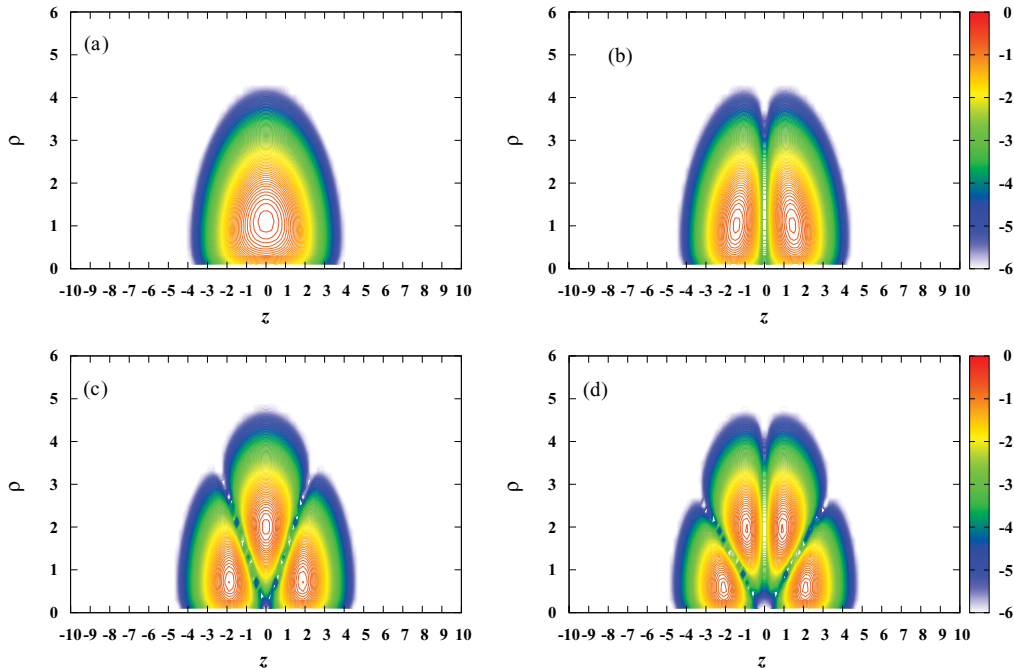


FIG. 2. (Color online) Probability densities for various modes of a Na condensate in an isotropic magnetic trap with $f_\rho = 25$ Hz and $f_z = 25$ Hz. (a) Ground mode at $\epsilon = 0.00$, (b) dipole mode at $\epsilon = 1.00$, (c) tripole mode at $\epsilon = 1.64$, and (d) quadrupole mode at $\epsilon = 2.35$ (cylindrical coordinates are in scaled units of $l = 4.19 \times 10^{-4}$ cm).

with energy $E_0 = 2.74$. We then propagated the GP equation in real time, as given by Eq. (12). With the same time-dependent Bragg scattering potential as used before with $\bar{\omega}_L = 1.0$, we obtained $E(10T) = 7.19$, in agreement with the cylindrical coordinate result in Fig. 1.

Upon diagonalization of the BdG matrix of Eq. (7) in cylindrical coordinates for $f_\rho = 25$ Hz and $f_z = 25$ Hz, we obtain a ground mode of eigenenergy $\epsilon = 0.0$ and a number of various types of modes at higher eigenenergies. The probability densities for selected modes of a Na condensate are presented in Fig. 2. The dipole mode in Fig. 2(b) at an eigenenergy of $\epsilon = 1.0$ is the mode being excited by the Bragg scattering calculations near $\bar{\omega}_L = 1.0$.

Upon relaxation of the GP equation in imaginary time for a nonisotropic magnetic trap with $f_\rho = 25$ Hz and $f_z = 10$ Hz, we obtain a ground state with energy $E_0 = 2.00$. We then propagated the GP equation in real time with a Bragg scattering potential of Eqs. (13)–(15), $\bar{A} = 0.10$, and $\bar{q}_L = 0.40$. We varied the Bragg scattering frequency $\bar{\omega}_L$ from 0.35 to 0.45 and kept track of the energy of Eq. (16). We present the results for $E(5T)$ and $E(10T)$ as a function of $\bar{\omega}_L$ in Fig. 3. Clearly, there is a resonance around $\bar{\omega}_L = 0.40$, and the energy becomes more sharply peaked for longer pulse durations.

In Cartesian coordinates, we chose a nonisotropic magnetic trap with $f_x = f_y = 25$ Hz and $f_z = 10$ Hz. Relaxation of the GP equation in imaginary time yielded an energy of $E_0 = 2.00$, while propagation of the GP equation in real time with $\bar{\omega}_L = 0.40$ yielded an energy of $E(10T) = 3.78$, both energies in agreement with the cylindrical coordinate results.

Upon diagonalization of the BdG matrix of Eq. (7) in cylindrical coordinates for $f_\rho = 25$ Hz and $f_z = 10$ Hz, we obtained a ground mode and various types of excited modes. The probability densities for selected modes of a Na

condensate are presented in Fig. 4. The dipole mode in Fig. 4(b) at an eigenenergy of $\epsilon = 0.40$ is the mode being excited by the Bragg scattering calculations near $\bar{\omega}_L = 0.40$.

We then propagated the GP equation in real time with a Bragg scattering potential of Eqs. (13)–(15) with $\bar{A} = 0.10$ to hunt for the tripole mode at $\epsilon = 0.69$ and the quadrupole mode at $\epsilon = 1.01$, as seen in Figs. 4(c) and 4(d). For $\bar{q}_L = 1.0$, we carried out nine calculations varying ω_L from 0.66 to 0.74 and an additional nine calculations varying ω_L from 0.92 to 1.08. The peaking of the energy seen in Fig. 3 around the dipole mode at $\epsilon = 0.40$ was not found in the energies near the tripole

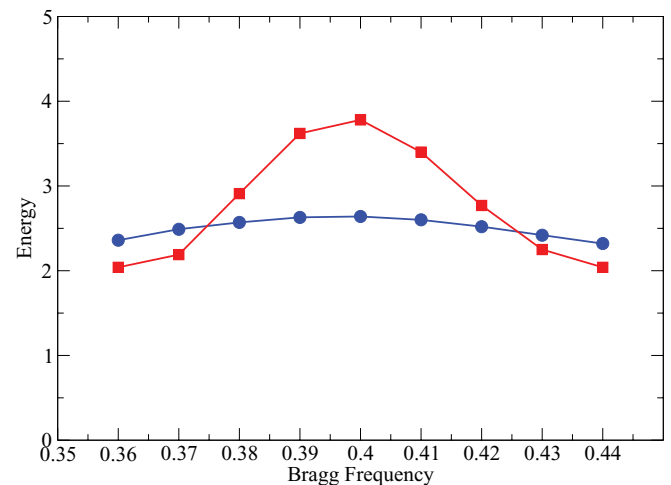


FIG. 3. (Color online) Photoexcitation of a Na condensate in a nonisotropic magnetic trap with $f_\rho = 25$ Hz and $f_z = 10$ Hz. Circles: Energy at $t = 5T$. Squares: Energy at $t = 10T$ (energies and frequencies are in scaled units of $\hbar\omega_\rho = 1.03 \times 10^{-13}$ eV).

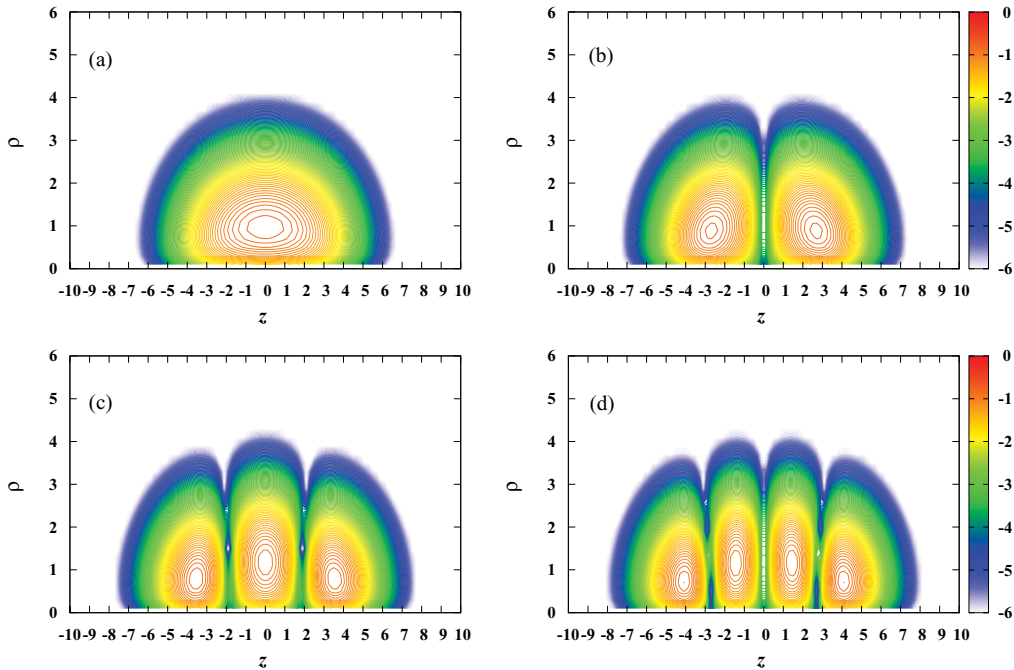


FIG. 4. (Color online) Probability densities for various modes of a Na condensate in a nonisotropic magnetic trap with $f_\rho = 25$ Hz and $f_z = 10$ Hz. (a) Ground mode at $\epsilon = 0.00$, (b) dipole mode at $\epsilon = 0.40$, (c) tripole mode at $\epsilon = 0.69$, and (d) quadrupole mode at $\epsilon = 1.01$ (cylindrical coordinates are in scaled units of $l = 4.19 \times 10^{-4}$ cm).

and quadrupole modes. We note that symmetry considerations preclude the dipole excitation of the tripole mode and overlap factors must significantly reduce the dipole excitation of the quadrupole mode.

IV. Summary. In summary, we have investigated the photoexcitation of a Na Bose-Einstein condensate by direct solution of the GP equation in both cylindrical and Cartesian coordinates with a time-dependent Bragg scattering potential. Dipole resonances were mapped out for Na condensates in both isotropic and nonisotropic magnetic traps by monitoring the time-dependent energy as the Bragg scattering frequency was varied. The dipole mode frequencies were

verified by diagonalization of the BdG matrix in cylindrical coordinates.

In the future, we plan to study the photoexcitation of other alkali-metal-atom condensates in various types of magnetic traps. We also plan to extend our photoexcitation studies to multispecies condensates.

Acknowledgments. This work was supported in part by grants from the US National Science Foundation. Computational work was carried out at the National Institute for Computational Sciences in Knoxville, Tennessee, and at the National Energy Research Scientific Computing Center in Oakland, California.

-
- [1] P. G. Burke, *R-Matrix Theory of Atomic Collisions* (Springer, Heidelberg, 2011).
- [2] M. M. Sant'Anna, A. S. Schlachter, G. Öhrwall, W. C. Stolte, D. W. Lindle, and B. M. McLaughlin, *Phys. Rev. Lett.* **107**, 033001 (2011).
- [3] M. Tashiro, *J. Chem. Phys.* **132**, 134306 (2010).
- [4] E. P. Gross, *Nuovo Cimento* **20**, 454 (1961).
- [5] L. P. Pitaevskii, *Zh. Eksp. Teor. Fiz.* **40**, 646 (1961) [*Sov. Phys. JETP* **13**, 451 (1961)].
- [6] P. B. Blakie and R. J. Ballagh, *Phys. Rev. Lett.* **86**, 3930 (2001).
- [7] T. P. Simula, N. Nygaard, S. X. Hu, L. A. Collins, B. I. Schneider, and K. Molmer, *Phys. Rev. A* **77**, 015401 (2008).
- [8] J. Steinhauer, N. Katz, R. Ozeri, N. Davidson, C. Tozzo, and F. Dalfovo, *Phys. Rev. Lett.* **90**, 060404 (2003).
- [9] S. R. Muniz, D. S. Naik, and C. Raman, *Phys. Rev. A* **73**, 041605 (2006).
- [10] J. M. Pino, R. J. Wild, P. Makotyn, D. S. Jin, and E. A. Cornell, *Phys. Rev. A* **83**, 033615 (2011).
- [11] M. Kozuma, L. Deng, E. W. Hagley, J. Wen, R. Lutwak, K. Helmerson, S. L. Rolston, and W. D. Phillips, *Phys. Rev. Lett.* **82**, 871 (1999).
- [12] Y. B. Band, M. Trippenbach, J. P. Burke, and P. S. Julienne, *Phys. Rev. Lett.* **84**, 5462 (2000).
- [13] M. S. Pindzola and B. Sun, *J. Phys. B* **43**, 235302 (2010).
- [14] N. Bogoliubov, *J. Phys. USSR* **11**, 23 (1947).
- [15] P. G. de Gennes, *Superconductivity of Metals and Alloys* (Benjamin, New York, 1966).
- [16] A. Fetter, *Ann. Phys. NY* **70**, 67 (1972).